

^{55}Mn NQR/NMR studies of the magnetic properties of YMn_2 under pressure

Guo-qing Zheng,* K. Nishikido, K. Ohnishi, Y. Kitaoka, and K. Asayama

Department of Physical Science, Graduate School of Engineering Science, Osaka University, Toyonaka, Osaka 560-8531, Japan

R. Hauser

Institut für Experimentalphysik, Technische Universität Wien, A-1040 Wien, Austria

(Received 1 December 1998)

We report magnetic properties of the antiferromagnet YMn_2 as functions of pressure and temperature (T) obtained from the ^{55}Mn spin-lattice relaxation rate and the Knight shift. An energy-band narrowing due to electron correlation is indicated by the Knight shift measurement and the application of pressure is found to enhance the conduction electron bandwidth. In the pressure-induced paramagnetic state, the system undergoes a crossover from an itinerant spin fluctuation (SF) regime at low T to a local SF regime at high T . It is pointed out that this magnetic crossover of SF resembles that of high-temperature superconductors. [S0163-1829(99)06921-0]

Spin fluctuations (SF's) in metals close to a magnetic instability (MI) have been studied extensively over the past two decades or so. In recent years, the subject of itinerant electron magnetism in transition-metal compounds has attracted new attention in connection with high-temperature superconducting Cu oxides (high- T_c cuprates) and heavy-fermion (HF) systems. High- T_c superconductivity occurs in the vicinity of magnetically ordered state and the antiferromagnetic (AF) spin fluctuation of Cu spins plays a central role in determining the anomalous properties in the normal state.¹ Such AF spin fluctuations may also play an important part in the occurrence of superconductivity.^{2,3} Nuclear magnetic resonance (NMR) measurements in the cuprates near an optimal doping show that the higher T_c is accompanied by a larger characteristic energy of AF spin fluctuation with a substantial magnetic correlation length.⁴ In the $4f$ or $5f$ HF systems, superconductivity is also found when the AF ordered state is suppressed by pressure.⁵ These properties suggest that the interplay between spin fluctuations and superconductivity may exist in wide classes of materials. It is therefore interesting to investigate the SF spectrum near the MI in materials besides the abovementioned ones.

YMn_2 is one of the candidate systems for this study. It crystallizes in the cubic C15 Laves phase structure where the Mn atoms form a sublattice of corner sharing tetrahedra while the Y atoms form the diamond sublattice. At ambient pressure, there is a first-order AF transition at $T_N \approx 100$ K.⁶ The AF order is easily suppressed by applying hydrostatic pressure or by chemical substitution at the Y sites (chemical pressure). Neutron scattering measurements on a Sc-substituted powder sample have found a magnetic response around the AF wave vector $Q = 1.5 \text{ \AA}^{-1}$.⁷ A recent neutron experiment on a $\text{Y}_{0.97}\text{Sc}_{0.03}\text{Mn}_2$ single crystal has revealed a wave-vector-dependent SF in the paramagnetic state at $T = 10$ K.⁸ Also, YMn_2 shows heavy-fermion-like behavior. Its electronic specific heat coefficient γ is $140 \text{ mJ K}^{-2} \text{ mol}^{-1}$ in Sc-substituted material⁹ and under pressure,¹⁰ which is larger by one order of magnitude than that of ordinary d -electron systems including high- T_c cu-

prates. The ratio A/γ^2 , where A is the coefficient of the quadratic contribution to the electric resistivity, is also close to that for heavy fermions.¹¹

In this paper we report an investigation of the magnetic properties of YMn_2 using nuclear quadrupole resonance (NQR) and NMR measurements under pressure up to 12 kbar. The main advantage of applying hydrostatic pressure is that it does not bring about crystal disorder or randomness which may complicate the investigation. It is also beneficial in that it is possible to finely tune the SF spectrum by varying the applied pressure. The polycrystal sample was prepared by an arc-melting method described elsewhere.¹² A clamped piston-cylinder device which was used in the previous study of high- T_c materials¹³ was adopted to generate pressure, which was calibrated by measuring the superconducting transition temperature of tin. The pressure inhomogeneity determined from the broadening of NQR spectrum of Cu_2O (Ref. 14) and CeCu_2Ge_2 (Ref. 15) is about ± 0.10 kbar. The rate $1/T_1$ was uniquely determined by fitting the nuclear magnetization recovery curve to the equation¹⁶

$$\frac{M(\infty) - M(t)}{M(\infty)} = \frac{3}{7} \exp\left(-\frac{3t}{T_1}\right) + \frac{4}{7} \exp\left(-\frac{10t}{T_1}\right).$$

We first remark on the transition from the AF ordered state to the paramagnetic state. At ambient pressure, the NMR spectrum has a well-resolved structure due to the quadrupolar interaction. T_N is ~ 50 and ~ 85 K in the cooling and heating process, respectively. Below T_N , it abruptly broadens and eventually disappears because of the internal magnetic field that develops. At $P \geq 4.0$ kbar, the well-resolved NMR spectrum remained down to 4.2 K, the lowest temperature at which the experiments were done. Moreover, the NQR signal was observed at 4.2 K, indicating that the system is in the pressure-induced paramagnetic state (PIPS). At $P = 3.3$ kbar, we found a coexistence of the AF ordered state and the PIPS. The AF state was confirmed by the sudden broadening of the NMR spectrum below T_N shown in

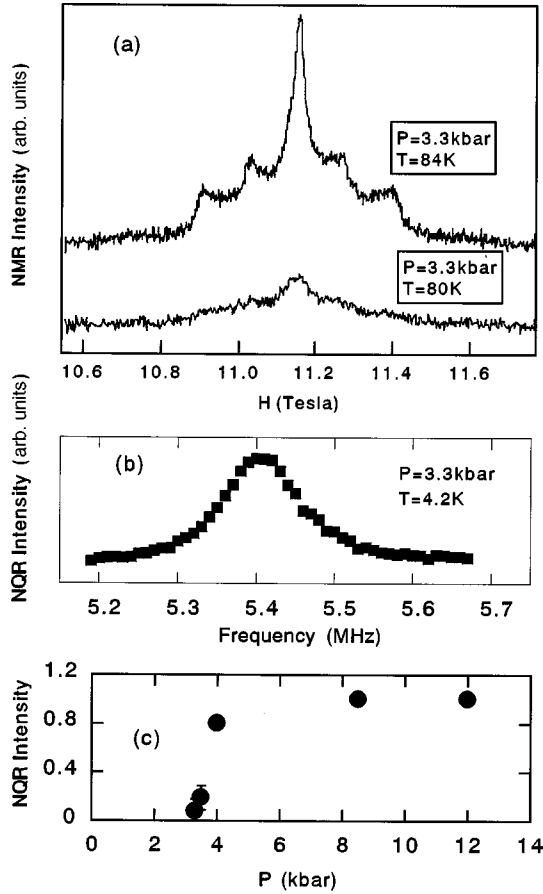


FIG. 1. (a) ^{55}Mn NMR spectra in YMn_2 above and below T_N with increasing T . (b) An example of the ^{55}Mn NQR spectrum of the $\pm 3/2 \leftrightarrow \pm 5/2$ transition at 4.2 K. (c) Relative NQR intensity after T_2 correction vs pressure.

Fig. 1(a). The PIPS was identified by the observation of the NQR signal at $T=4.2$ K [Fig. 1(b)] and above. As seen in Fig. 1(c), the NQR intensity was reduced below $P=4.0$ kbar, suggesting that the AF state and the PIPS coexist in a wide pressure range which cannot be ascribed to the pressure inhomogeneity. The volume fraction of the PIPS at $P=3.3$ kbar is estimated to be 10% of the total from the NQR intensity and T_N of the remaining AF state at $P=3.3$ kbar does not change from that at ambient pressure. The lack of change in T_N and the coexistence of the AF and PIPS suggest strongly that the pressure-induced phase transition is of the first order. This result also seems to explain why the critical pressure reported from different experiments is so widely scattered from 2.7 to 3.7 kbar.^{12,17,18}

The static properties are shown by the T dependence of the ^{55}Mn Knight shift K for $P=1$ bar, 3.3 kbar, and 8.5 kbar in Fig. 2. In general, $K=K_s+K_{\text{orb}}=A_{\text{orb}}\chi_{\text{orb}}^{\text{Mn}}+A_s\chi_s^{\text{Mn}}$, where K_s is the spin part, K_{orb} is the orbital part, $\chi_{\text{orb}}^{\text{Mn}}$ and χ_s^{Mn} are the Mn orbital and spin susceptibility, respectively, and $A_{\text{orb},s}$ are the hyperfine coupling constants. The observed susceptibility can be decomposed as $\chi_{\text{obs}}^{\text{Mn}}=\chi_s^{\text{Mn}}+\chi_{\text{orb}}^{\text{Mn}}+\chi_{\text{dia}}$, where χ_{dia} is the diamagnetic susceptibility due to closed shells of Y and Mn. We ignore other contributions from yttrium which are much smaller compared to Mn.¹⁹ From the good fit of K vs χ seen in the inset of Fig. 2, we obtain $A_s=-194$ kOe/ μ_B , $K_{\text{orb}}=1.23\%$, and $\chi_s^{\text{Mn}}=\chi_{\text{obs}}^{\text{Mn}}$

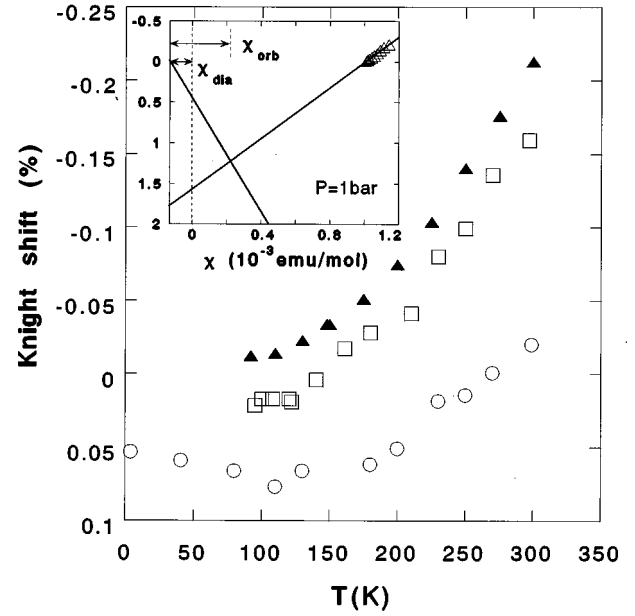


FIG. 2. ^{55}Mn Knight shift in YMn_2 . Closed triangles: $P=1$ bar, squares: $P=3.3$ kbar, circles: $P=8.5$ kbar. The inset shows the K vs χ plot for $P=1$ bar.

$-\chi_{\text{dia}}-\chi_{\text{orb}}^{\text{Mn}}=0.80 \times 10^{-3}$ emu/(mol YMn_2) at $T=110$ K at ambient pressure. Here we have used χ_{obs} of Ref. 7, $A_{\text{orb}}=390$ kOe/ μ_B (Ref. 20) and $\chi_{\text{dia}}=-0.125 \times 10^{-3}$ emu/mol.²¹ The obtained A_s and K_{orb} are comparable to those for liquid manganese.²² By the relation of $N(E_F)=\chi_s^{\text{Mn}}/2\mu_B^2$, the density of states (DOS) at the Fermi level $N(E_F)$ was calculated as 12.4 states/(eV YMn_2 spin). This value is larger by a factor of 5 than that of the band calculation,¹⁹ which indicates band narrowing by electron correlations. The large $N(E_F)$ accounts partially for the large γ of this system. As seen in Fig. 2, upon increasing the pressure the Knight shift is increased, which indicates a decrease of χ_s^{Mn} because the hyperfine coupling constant is negative. This shows that the pressure increases the band width. Since the lattice expands upon heating,⁷ the T dependence of K above $T=130$ K can also be attributed to a change in bandwidth.

We next turn to the character of SF in the PIPS. Figure 3 shows that $1/T_1$ increases with increasing T , but then becomes almost independent of T at high T . Let us compare this characteristic SF with that found in the neutron scattering experiment for $\text{Y}_{0.97}\text{Sc}_{0.03}\text{Mn}_2$ at $T=10$ K. Ballou *et al.*⁸ found that the SF in this alloy is highly anisotropic because of frustration associated with the tetrahedral coordination of the Mn atoms. The Mn spin correlation length ξ is 2.86 Å, which is about the distance between the nearest Mn atoms along [110] direction, while ξ is only 1.72 Å along the [001] direction. Lacroix *et al.*²³ have developed an extended SCR theory to explain the low- T SF character found by the neutron experiment and predicted that $1/T_1T$ should vary as $\chi_Q^{3/4}$ where χ_Q is the staggered susceptibility at AF wave vector Q . One may think this prediction as a consequence of the decrease in the dimensionality, since in three-dimensional (3D) systems $1/T_1T \propto \chi_Q^{1/2}$ and in 2D systems $1/T_1T \propto \chi_Q$.³ In the case of strong AF spin fluctuation, $1/T_1$ is

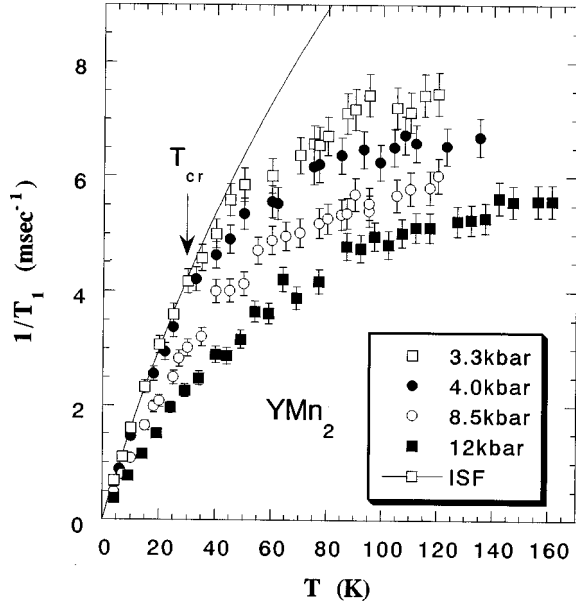


FIG. 3. Temperature dependence of $1/T_1$ for ^{55}Mn in YMn_2 at four pressures. The solid curve is a fit of the $P=3.3$ kbar data to the theory of itinerant spin fluctuations and T_{cr} is the temperature at which it ceases to fit the data.

dominated by χ_Q , which follows the Curie-Weiss type T dependence,³ therefore $1/T_1 T \propto \chi_Q^{3/4} \propto 1/(T + \theta)^{3/4}$. However, we found that no single curve of the predicted form can fit the data of the *whole* T range, nor a 3D function. The curve in Fig. 3 is a fit of the data at $P=3.3$ kbar below 40 K to Lacroix's equation. One finds that the high- T data cannot be described by the theoretical curve. This deviation from the itinerant spin fluctuation (ISF) model is better seen in Fig. 4 where $(T_1 T)^{4/3}$ is plotted vs T and the solid lines indicate the relation of $(T_1 T)^{4/3} \propto T + \theta$. The data deviates from the theoretical line around $T \leq 40$ K, for all four pressures. We propose that $1/T_1$ in the high- T region is dominated by localized moments, where $1/T_1$ is given by

$$\frac{1}{T_1} = \frac{\gamma_n^2}{2} \frac{S(S+1)}{3} \frac{A_s^2}{\omega_c},$$

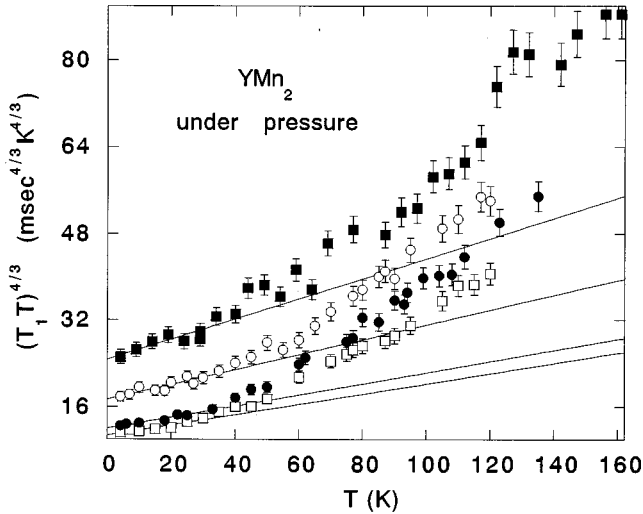


FIG. 4. $(T_1 T)^{4/3}$ plotted versus T . The solid lines indicate the $(T_1 T)^{4/3} \propto T + \theta$ relation. The symbols are the same as for Fig. 3.

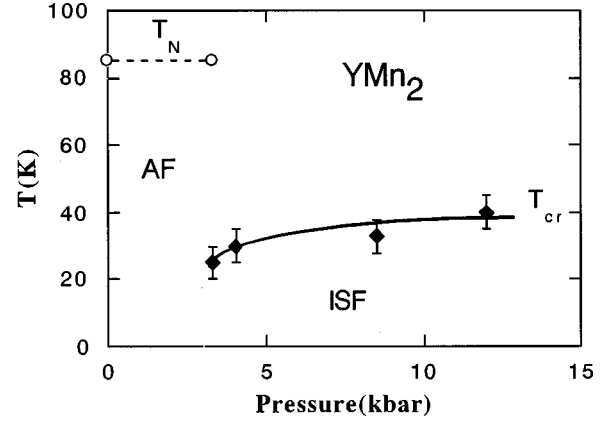


FIG. 5. Pressure-temperature phase diagram for YMn_2 . Below $P \approx 3.3$ kbar and $T = 80$ K, the system is in the antiferromagnetically (AF) ordered state. Above $P \approx 3.3$ kbar and below T_{cr} the system is in the itinerant spin fluctuation (ISF) state. There is a coexistence of AF and ISF states around $P = 3.3$ kbar (see text).

with S being the effective spin moment and ω_c the correlation frequency.²⁴ A possible origin of the seemingly localized moment may be that the T -dependent mean squared local amplitude of the spin density $\langle S^2 \rangle$ is saturated at high temperatures. Such a thermally induced local moment has been argued theoretically^{25,23} and experimental support was also reported.²⁶ Note that the magnitude of the saturated $1/T_1$ at high T decreases with increasing pressure. This may be attributed to the reduction of $\langle S^2 \rangle$ by pressure. It is probably because the itinerancy of d electrons is increased by the mixing between the d and s electrons and/or by the direct overlapping of d electrons. This is consistent with the Knight shift result that indicates the bandwidth enhancement by the pressure. It is also consistent with resistivity (ρ) measurement where ρ becomes constant at high T and its magnitude decreases as pressure increases.¹² From the low- T behavior of $1/T_1$, we find the parameter θ to be -113 , -117 , -126 , and -133 K for $P = 3.3$, 4.0, 8.5, and 12 kbar, respectively, by fitting the data of Fig. 4 below 40 K to the ISF equation. This is consistent with the system being moved away from the MI when pressure is increased. Lacroix *et al.*²³ have discussed the proximity of $(\text{Y}_{0.97}\text{Sc}_{0.03})\text{Mn}_2$ to the MI, based on the neutron data. They estimated θ to be 170 K. The smaller θ found in the present study suggests that the pure system even at $P = 12$ kbar is still closer to the MI than $(\text{Y}_{0.97}\text{Sc}_{0.03})\text{Mn}_2$ is, although the quadrupole frequency ν_Q for $\text{Y}_{0.97}\text{Sc}_{0.03}\text{Mn}_2$ (Ref. 27) is close to $\nu_Q = 5.42$ MHz at $P = 4.0$ kbar of the pure system which increases at a rate of 9.8 kHz/kbar.

Thus, we find that *the PIPS of YMn_2 undergoes a crossover from the itinerant SF regime at low T to a different regime at high T which appears to be governed by localized SF.* We define the crossover temperature T_{cr} at which the data deviates from the theoretical line. As seen in the phase diagram of Fig. 5, T_{cr} is not so sensitive to pressure. A comparison of the crossover in the T dependence of $1/T_1$ with the resistivity under pressure shows a characteristic temperature T_{sf} , below which the resistivity exhibits a T^2 variation.¹² T_{sf} was found to be about 22 K at a pressure of 4.2 kbar, which is quite close to $T_{\text{cr}} = 30$ K at 4.0 kbar found in this study.

We believe that these two characteristic temperatures are related to the common crossover temperature of SF found here.

The crossover in the electronic state of Y Mn_2 resembles that of high- T_c cuprates^{28,29} and the heavy fermions.³⁰ In the latter system a similar crossover from an ISF regime to a localized SF regime also takes place. T_{cr} in the present material is on the same order as that in HF systems but is lower than that in the cuprates by one order of magnitude. For instance, in $\text{La}_{2-x}\text{Sr}_x\text{CuO}_4$ ($x \leq 0.15$), $1/T_1 T$ follows a Curie-Weiss type T dependence below 300 K (Ref. 28) but $1/T_1$ saturates at high temperatures.²⁹ The stronger localized character of Y Mn_2 than the cuprates can be attributed to its narrow band and the short magnetic correlation length. We estimate that the band width in Y Mn_2 is approximately by one order of magnitude smaller than that of the high- T_c cuprates based upon the DOS at the Fermi surface. On the other hand, the magnetic correlation length ξ in Y Mn_2 is less than the Mn-Mn distance. By contrast, the Cu AF spin correlation in cuprates is extended over several lattice constants, i.e., $\xi \sim 3a$ in lightly doped material $\text{La}_{1.85}\text{Sr}_{0.15}\text{CuO}_4$ (Ref. 31) and $\xi \sim 2a$ at T_c in cuprates around the optimal doping level,^{2,4} where a is the Cu-Cu distance. It has been proposed that for SF mediated superconductivity, a larger bandwidth

with a larger ξ favors a higher T_c .^{2,3} According to this proposal, Y Mn_2 is unfavorable for superconductivity compared to the cuprates. Nevertheless, it is worthwhile to search for superconductivity through tuning SF by varying pressure so as to increase the band width while keeping ξ finite.

In summary, we have studied the magnetic properties of Y Mn_2 as functions of pressure and temperature by ^{55}Mn NQR/NMR techniques. From the Knight shift, it was proposed that the energy band is narrowed due to electron correlation, and the effect of pressure is to enhance the itinerancy of Mn d electrons, resulting in the increase of the band width. In the pressure-induced paramagnetic state, the system undergoes a crossover from an itinerant spin fluctuation (SF) regime at low T to a seemingly local SF regime at high T . The magnetic crossover of SF in Y Mn_2 resembles that of high- T_c cuprates.

We thank M. Shirai for helpful discussions, T. Moriya and M. Shiga for comments, and W.G. Clark for a critical reading of the manuscript. This work was supported in part by grants-in-Aid for Scientific Research from the Ministry of Education, Science and Culture, Japan, under Grant Nos. 09740284 and 10CE2004.

*Electronic address: zheng@mp.es.osaka-u.ac.jp

¹See, for example, *Physical Properties of High- T_c Superconductors*, edited by D. M. Ginzburg (World Scientific, Singapore, 1990).

²D. Monthoux and D. Pines, *Phys. Rev. B* **49**, 4261 (1994).

³T. Moriya, K. Ueda, and Y. Takahashi, *J. Phys. Soc. Jpn.* **59**, 290 (1990); T. Moriya and K. Ueda, *ibid.* **63**, 1871 (1994).

⁴G.-q. Zheng, Y. Kitaoka, K. Asayama, K. Hamada, H. Yamauchi, and S. Tanaka, *J. Phys. Soc. Jpn.* **64**, 3184 (1995); K. Magishi, G.-q. Zheng, Y. Kitaoka, K. Asayama, K. Tokiwa, A. Iyo, and H. Ihara, *ibid.* **64**, 4561 (1995); G.-q. Zheng, Y. Kitaoka, K. Asayama, K. Hamada, H. Yamauchi, and S. Tanaka, *Physica C* **260**, 197 (1996).

⁵F. M. Grosche, S. R. Julian, N. D. Mathur, and G. G. Lozarich, *Physica B* **223&224**, 50 (1996); R. Movshovich, T. Graf, D. Mandrus, M. F. Hundley, J. D. Thompson, R. A. Fisher, N. E. Phillips, and J. L. Smith, *ibid.* **223&224**, 126 (1996).

⁶For an overview of Y Mn_2 , see M. Shiga, *Physica B* **149**, 293 (1988).

⁷M. Shiga, H. Wada, Y. Nakamura, J. Deportes, B. Ouladdiaf, and K. R. Ziebeck, *J. Phys. Soc. Jpn.* **57**, 3141 (1988).

⁸R. Ballou, E. Lelievre-Berna, and B. Fak, *Phys. Rev. Lett.* **76**, 2125 (1996).

⁹H. Wada, H. Nakamura, E. Fukami, K. Yoshimura, M. Shiga, and Y. Nakamura, *J. Magn. Magn. Mater.* **70**, 17 (1987).

¹⁰R. A. Fisher, R. Ballou, J. P. Emerson, E. Lelievre-Berna, and N. E. Phillips, *Int. J. Mod. Phys. B* **7**, 830 (1993).

¹¹R. Hauser, E. Bauer, E. Gratz, I. S. Dubenko, and A. S. Markosyan, *Physica B* **199&200**, 662 (1994).

¹²R. Hauser, E. Bauer, E. Gratz, Th. Haufler, G. Hilscher, and G. Wiesinger, *Phys. Rev. B* **50**, 13 493 (1994).

¹³G.-q. Zheng, E. Yanase, Y. Kitaoka, K. Ishida, K. Asayama, Y. Kodama, R. Tanaka, and S. Endo, *Solid State Commun.* **79**, 51 (1991).

¹⁴A. P. Reyes, E. T. Ahrens, R. H. Heffner, P. C. Hammel, and J. D. Thompson, *Rev. Sci. Instrum.* **63**, 3120 (1992).

¹⁵G.-q. Zheng *et al.* (unpublished).

¹⁶A. Narath, *Phys. Rev.* **162**, 320 (1967).

¹⁷G. Oomi, T. Terada, M. Shiga, and Y. Nakamura, *J. Magn. Magn. Mater.* **70**, 137 (1987).

¹⁸S. Mondal, R. Cywinski, S. H. Kilcoyne, B. D. Rainford, and C. Ritter, *Physica B* **180&181**, 108 (1992).

¹⁹H. Yamada, J. Inoue, K. Terao, S. Kanda, and M. Shimizu, *J. Phys. F* **14**, 1943 (1984).

²⁰A. Freeman and R. Watson, in *Magnetism IIA*, edited by H. Suhl and G. Rado (Academic, New York, 1965), p. 168.

²¹G. C. Carter, L. H. Bennett, and D. J. Kahan, *Metallic Shifts in NMR* (Pergamon, Oxford, 1977), p. 5.

²²W. W. Warren and U. El-Hanany, *J. Phys. C* **4**, 337 (1974).

²³C. Lacroix, A. Solontsov, and R. Ballou, *Phys. Rev. B* **54**, 15 178 (1996).

²⁴T. Moriya, *J. Phys. Soc. Jpn.* **18**, 516 (1963).

²⁵T. Moriya, *Solid State Commun.* **26**, 483 (1978); A. Inagaki and T. Moriya, *J. Phys. Soc. Jpn.* **67**, 3924 (1998).

²⁶N. Inoue and Y. Yasuoka, *Solid State Commun.* **30**, 341 (1979).

²⁷H. Nakamura, Y. Kitaoka, K. Yoshimura, Y. Kohori, K. Asayama, M. Shiga, and Y. Nakamura, *J. Phys. (Paris)* **49**, C8-257 (1988).

²⁸S. Ohsugi, Y. Kitaoka, K. Ishida, G.-q. Zheng, and K. Asayama, *J. Phys. Soc. Jpn.* **63**, 700 (1994).

²⁹T. Imai, C. P. Slichter, K. Yoshimura, and K. Kosuge, *Phys. Rev. Lett.* **70**, 1002 (1993).

³⁰For example, Y. Kitaoka, K. Ueda, T. Kohara, K. Asayama, Y. Ohnuki, and T. Komatsubara, *J. Magn. Magn. Mater.* **52**, 341 (1985).

³¹S. M. Hayden, G. Aeppli, H. A. Mook, T. G. Perring, T. E. Mason, S.-W. Cheong, and Z. Fisk, *Phys. Rev. Lett.* **76**, 1344 (1996).